New Journal of Physics
The open-access journal for physics

Ultrabright and efficient single-photon generation based on nitrogen-vacancy centres in nanodiamonds on a solid immersion lens

Tim Schröder[1], Friedemann Gädeke, Moritz Julian Banholzer and Oliver Benson

Humboldt-Universität zu Berlin, Institut für Physik, AG Nano Optics
Newtonstraße 15, 12489 Berlin, Germany
E-mail: tim.schroeder@physik.hu-berlin.de

New Journal of Physics **13** (2011) 055017 (9pp)
Received 5 November 2010
Published 26 May 2011
Online at http://www.njp.org/
doi:10.1088/1367-2630/13/5/055017

Abstract. Single photons are fundamental elements for quantum information technologies such as quantum cryptography, quantum information storage and optical quantum computing. Colour centres in diamond have proven to be stable single-photon sources and thus essential components for reliable and integrated quantum information technology. A key requirement for such applications is a large photon flux and a high efficiency. Paying tribute to various attempts to maximize the single-photon flux, we show that collection efficiencies of photons from colour centres can be increased with a rather simple experimental setup. To do so, we spin-coated nanodiamonds containing single nitrogen-vacancy (N-V) colour centres on the flat surface of a ZrO_2 solid immersion lens. We found stable single-photon count rates of up to 853 kcts s^{-1} at saturation under continuous wave excitation while having access to more than 100 defect centres with count rates from 400 to 500 kcts s^{-1}. For a blinking defect centre, we found count rates up to 2.4 Mcts s^{-1} for time intervals of several tens of seconds. It seems to be a general feature that very high rates are accompanied by blinking behaviour. The overall collection efficiency of our setup of up to 4.2% is the highest yet reported for N-V defect centres in diamond. Under pulsed excitation of a stable emitter of 10 MHz, 2.2% of all pulses caused a click on the detector adding to 221 kcts s^{-1} thus, opening the way towards diamond-based on-demand single-photon sources for quantum applications.

[1] Author to whom any correspondence should be addressed.

Increased single-photon collection with high on-demand efficiency allows higher communication bit rates in quantum cryptography [1] and faster readout of stationary qubits [2, 3]. Also, a key operation in quantum information processing (QIP), i.e. two-photon interference, requires a large photon flux. Advanced protocols, such as entanglement swapping or entanglement transfer [4, 5], are also not possible if photons as flying qubits cannot be generated or collected efficiently. A first crucial step concerns reliable single-photon generators. Such systems have been realized based on atoms [6, 7], ions [8], molecules [9] and solid-state-based emitters such as quantum dots [10] or defect centres in diamond [11]. There were also successful attempts at integrating solid-state emitters in photonic nanostructures to increase the photon flux [12–14]. In particular, defect centres in diamond have drawn much attention lately as they are photostable even at room temperature. Since the first demonstration that single photons can be collected from nitrogen-vacancy (N-V) defect centres in diamond more than 10 years ago [11], a steady improvement of collection rates has been achieved. Furthermore, other defect centres with different optical behaviour have been found and fabricated [15–17] in bulk as well as diamond nanocrystals. Nanodiamonds have several advantages compared with bulk diamond as they can be easily deposited on various substrates with e.g. spin-coating techniques or nanomanipulation. Atomic force microscope (AFM) manipulation has been used to integrate them on photonic crystal resonators [18] or on optical fibres [19]. Moreover, photon collection efficiency of nanodiamonds is generally higher [20]. Yet, it was shown just recently that a reduction of excitation intensity and an improvement of emission collection of N-V centres in bulk diamond can be achieved via etching adequate structures into chemical vapour deposition (CVD) grown bulk diamond [21–23]. Nanorods [21] or solid immersion lenses (SILs) [22, 23] facilitate the collection of single photons of up to 500 kcts s^{-1}. Unfortunately, fabrication of these structures demands rather sophisticated processes.

SILs, on the other hand, have been integrated into optical microscopes since 1990 [24] and are commercially available in various designs. A solid immersion lens can be formed as a simple half-sphere or in a so-called Weierstrass design [25] and is typically made of high-index material, e.g. ZrO_2 with $n = 2.17$. The operation principle of a SIL is very similar to that of an oil-immersion microscope. Samples are deposited either on or close to the flat side of the SIL, while the optical access lies on the curved side of the SIL. In this way, the wave front of a focused light beam passes the surface parallel and neither refraction nor aberration takes place. Due to the high index of refraction the numerical aperture (NA) is enhanced, providing larger collection angles and thus improved collection efficiency. Also the resolution is increased similarly to oil-immersion microscopes, and much higher energy densities in the focus are obtained [24]. With respect to the implementation of SILs with a single photon emitter, there is another important feature. Due to the strong step in the index of refraction at the SIL–air interface, the dipole emission is not symmetrically distributed into SIL and air, respectively [26]. We performed finite-difference time domain (FDTD) calculations for our specific system and found that a simple dipole emitter in air, 10 nm away from a flat material surface with $n = 2.17$, emits more than 86 % of its emission into the direction of the SIL if oriented parallel to the surface and more than 75 % if oriented perpendicular to the surface. These results are in agreement with an analytical analysis of a dipole emitter in front of a flat dielectric interface [27]. The combination of commercial availability, easy experimental integration, well increased NA, smaller focus and strongly enhanced emission into the direction of collection make a solid immersion lens a very potent tool to increase single photon emitter collection efficiencies.

Here, we present the experimental implementation of an SIL microscope combined with the advantages of nanodiamonds which outperform the so far reported single photon count

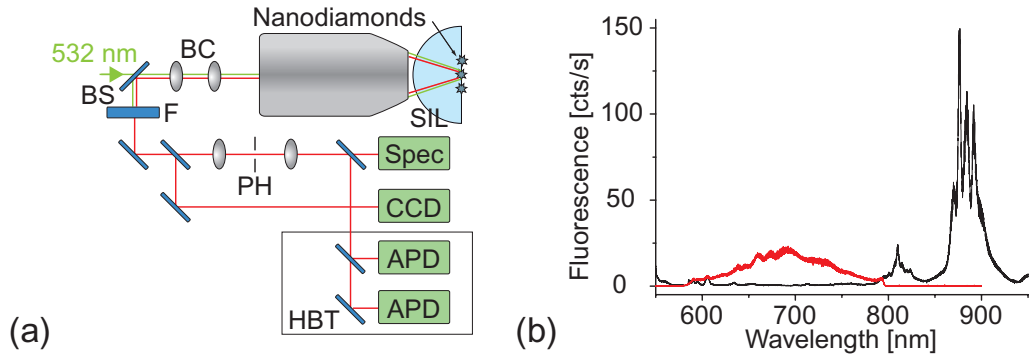

Figure 1. Experimental setup and spectroscopic properties of the solid immersion lens. (a) Sketch of a home-built confocal microscope. BC, BS, F, PH, HBT and APD stand for beam control, beam splitter, filter, pinhole, Hanbury-Brown and Twiss setup and avalanche photo diode, respectively. (b) Spectrum of the fluorescence from a solid immersion lens (black curve) at an excitation power of 933 μW and spectrum of an N-V centre on a SIL after filtering with a 590 nm long-pass and a 795 nm short-pass filter (red curve).

rates from N-V centres in diamond. By spin-coating nanodiamonds on the flat surface of commercially available ZrO_2 half-spheres (MIKROP, Switzerland) with a radius of 1 mm, we prepared a SIL suitable for efficiently exciting colour centres inside the nanodiamonds. The SIL was implemented into a home-built confocal microscope featuring an air objective with a NA of 0.9 (Mitutoyo, Japan) and a pinhole of 100 μm as depicted in figure 1(a). To reduce stray light from laser excitation and SIL fluorescence, 540 and 590 nm long-pass filters as well as a 795 nm short-pass filter were used. Via the spin-coating technique there is a wide flexibility to integrate nanodiamonds with arbitrary colour centres into any kind of SIL. The latter can be half-sphere SILs or Weierstrass SILs made of various materials transparent at excitation and colour centre emission wavelengths. The chosen material ZrO_2 has a high index of refraction n of 2.17 at 600 nm and can be processed to half-spheres within required tolerances [28]. At an excitation wavelength of 532 nm and a typical excitation power of less than 1 mW which is appropriate for defect centres in diamond, the intrinsic fluorescence of the SIL due to impurities is negligible between wavelengths of 615 and 785 nm (see the spectrum in figure 1(b)). It is thus well suited for the collection of photons from e.g. N-V centres [11], Ni/Si-related centres [29, 30] and Si-V centres [16, 31] emitting from 600 to 800 nm (see the spectrum of an N-V centre in figure 1(b)), around 770 nm and around 740 nm, respectively.

For spin-coating, we used an aqueous solution with 0.01% polyvinyl alcohol and nanodiamonds (Microdiamant, Switzerland, HPHT synthesis) with a mean size of 25 nm. Spin-coating of a solution with suitable diamond density was performed with 2000 rpm to ensure a dense distribution of the diamonds with distances smaller than 1 μm. Figure 2(a) shows an x–y-intensity scan of the confocal microscope of a 10 μm $\times$ 10 μm region with typical diamond distribution and fluorescence intensity. In a rectangular array of about 10 μm by 100 μm around the centre of the SIL at least ten diamonds showed count rates of more than 250 kcts s^{-1} when excited with 148 μW of a pulsed laser (Picoquant, Germany, 532 nm, pulse width about 110 ps) with a repetition rate of 80 MHz, whereas many more diamonds showed

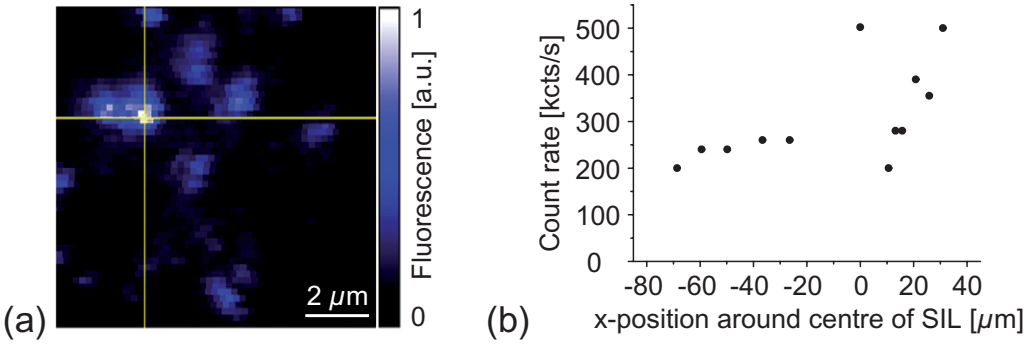

Figure 2. x–y-confocal fluorescence scan of nanodiamonds on an SIL and emission intensity of several N-V centres close to the SIL centre. (a) $10\,\mu\text{m} \times 10\,\mu\text{m}$ fluorescence intensity scan of an area close to the centre of the SIL. Such scans typically feature a few bright ($R_{\text{Inf}} = 400$–$700\,\text{kcts}\,\text{s}^{-1}$) and many darker ($R_{\text{Inf}} < 400\,\text{kcts}\,\text{s}^{-1}$) N-V centres. (b) Photon count rates of different N-V centres under pulsed excitation of 80 MHz and excitation intensities of $148\,\mu\text{W}$ in the focus. The count rates of 12 N-V centres along one scan direction (x-axis) across the centre of the flat SIL surface were investigated. All emitters provide single emitter characteristics proven by a measured value of the normalized second-order correlation function $g^{(2)}(0) < 0.5$.

count rates around $200\,\text{kcts}\,\text{s}^{-1}$ (see figure 2(b)). An excitation of 80 MHz represents quasi-CW excitation for N-V centres with a typical lifetime of 18 ns. It should be mentioned that many of the diamonds investigated showed blinking behaviour [32]. We extrapolated the count rates of the ten measured defect centres (see e.g. figure 3(a)) and derived saturation count rates under CW excitation between 400 and $500\,\text{kcts}\,\text{s}^{-1}$. For an area of $100\,\mu\text{m} \times 100\,\mu\text{m}$, we expect more than 100 colour centres with similar emission rates. This offers the opportunity to select suitable diamonds out of a large ensemble for special applications, e.g. a specific ultrabright diamond or two diamonds with matching zero phonon line emission for two-photon interference experiments.

To prove the single photon character of the light emitted from a specific colour centre under study, we carried out autocorrelation measurements in a Hanbury Brown and Twiss (HBT) setup (see figure 1(a)). If the normalized intensity autocorrelation function

$$g^{(2)}(\tau) = \frac{\langle I(t)\, I(t+\tau)\rangle}{\langle I(t)\rangle^2}$$

has values at zero time delay $\tau = 0$ of $g^{(2)}(0) < 0.5$, emission should occur basically from a single N-V centre. Typical $g^{(2)}(\tau)$ functions of the measured N-V centres have a $g^{(2)}(0)$ between 0.1 and 0.3, depending on excitation intensities. In order to determine the maximum accessible photon flux, we carried out saturation measurements (displayed in figures 3(a) and (b)). Fits to the experimental curves were done according to

$$R(I) = \frac{R_{\text{Inf}}\, I}{I_{\text{Sat}} + I} + (A + \alpha) I + \beta,$$

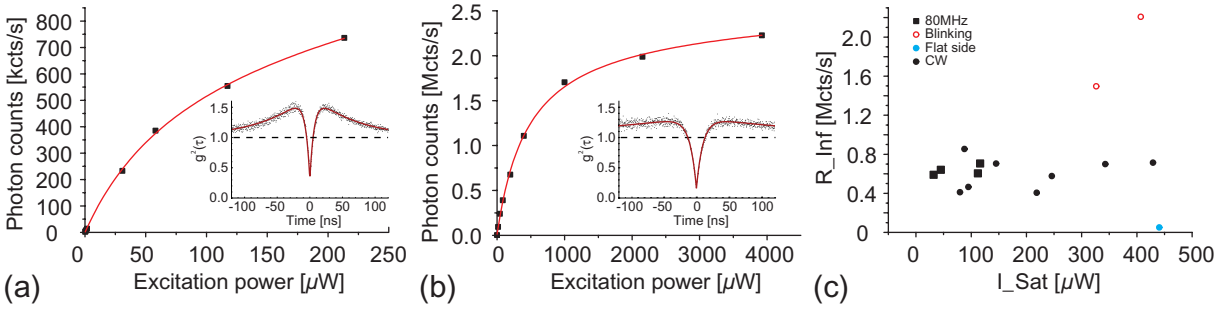

Figure 3. Autocorrelation and saturation measurements of different N-V centres. (a) Saturation measurement of the brightest stable emitter found. R_{Inf} is 853 kcts s^{-1}, while the saturation excitation intensity is 88 μW. The inset shows the normalized autocorrelation function $g^{(2)}(\tau)$ of the same emitter with $g^{(2)}(0) < 0.3$. (b) Saturation measurement of the brightest blinking emitter found. R_{Inf} is 2.4 Mcts s^{-1} on a time basis of several tens of seconds, while the saturation excitation intensity is 464 μW. The averaged count rate is 477 kcts s^{-1} for an excitation intensity of 2.6 mW. The inset shows the normalized autocorrelation function $g^{(2)}(\tau)$ of the same emitter with $g^{(2)}(0) < 0.16$ at an excitation of 1 mW. The red curves in (a) and (b) are theoretical fits to the data (see text). (c) Saturation count rates of different N-V centres plotted against the saturation excitation intensities. Black symbols represent stable emitters, open red circles represent blinking ones and the blue dot represents an N-V centre probed from the flat side of the SIL (the right side of the SIL in figure 1(a)). Square symbols denote quasi-CW excitation with 80 MHz laser repetition rate, while circles denote CW excitation.

where R is the single-photon count rate, R_{Inf} the count rate at infinite excitation intensities, I the excitation intensity, I_{Sat} the saturation excitation intensity and A represents the measured background fluorescence 1 μm away from the N-V centre, while α and β are fit parameters for linear background stemming from the diamond and additional background such as dark count from the avalanche photo diode (APD) and residual stray light, respectively. Most saturation excitation intensities were about 80 μW in the focus, while the typical single photon count rate R was 500 kcts s^{-1} without background substraction as can be seen in figure 3(c). Twelve single N-V centres of similar brightness were analysed. It should be pointed out, however, that these N-V centres have quite different saturation intensities as can be derived from figure 3(c). This is to some degree due to their randomly distributed dipole orientations. Furthermore, the nanodiamonds have mismatched physical and optical contact with the SIL surface, resulting in diverse optical coupling of the nanodiamonds to the SIL. In figure 3(c), also the count rate at saturation for an N-V centre that was probed from the air side of the SIL is depicted. This N-V centre, the brightest we found from the flat side, shows count rates at saturation of only 50 kcts s^{-1}, which is about ten times lower than typical count rates from centres excited through the SIL. Furthermore, its saturation intensity of 440 μW is also about five times higher.

We found one outstanding N-V centre with a stable single photon count rate at saturation of 853 kcts s^{-1}. Even at excitation intensities of 213 μW and count rates of 736 kcts s^{-1}, its $g^{(2)}(0)$ value was smaller than 0.3. In principle it could have been further reduced by adequate

filtering (see figure 1(b)). Furthermore, we observed another remarkable single defect centre. This defect centre was ultrabright, i.e. we found single photon count rates of up to 2.4 Mcts s^{-1} at saturation on a time base up to several tens of seconds alternating with darker periods. There was no pronounced on–off behaviour, but rather jumps between a very bright state and several states with far less intensity. On average, the single photon emission rate was 400 kcts s^{-1} at an excitation power of 2.6 mW. We also measured its autocorrelation function at count rates of up to 1.1 Mcts s^{-1} to be smaller than $g^{(2)}(0) < 0.16$. In our experiments, we found that in an ensemble of nanodiamonds there exist a few ultrabright defect centres with rates > 1 Mcts s^{-1}. However, this large rate seems to be accompanied by pronounced blinking behaviour. The reason for this is not yet understood. Photochromic behaviour may play a role. Compared with recent studies of blinking in very small (5 nm) nanodiamonds [32], the size of nanodiamonds we used is much larger. Yet, with defect centres located close to the surface the situation may be similar. As mentioned, there is first evidence that more than just two on- and off-states occur. Since there are typically only a few ultrabright blinking N-V defect centres, a solid statement concerning the reason for the blinking is not possible yet. However, the correlation of brightness and blinking warrants further studies.

For most applications of single photons in QIP, on-demand generation is required [33]. One possibility is to use pulsed excitation. A crucial parameter of such a source is the collection efficiency per excitation pulse. A perfect single photon on-demand device would deliver exactly one detected single photon per pulse in a well-defined optical mode. Such performance is limited in real devices mainly by the efficiency in collecting single photon emission with the first lens, losses in the optical path towards the detector as well as by detector efficiencies.

To determine the collection efficiency of our setup we measured the collection efficiency per excitation pulse. The repetition rate of the pulsed excitation laser was limited to about 10 MHz, such that the time interval between pulses was 100 ns, i.e. much larger than the lifetime of 18 ns of the N-V centre in figure 4(b). With these numbers the probability for excited N-V centres to decay before the arrival of the next exciting pulse was 0.97. If we further assume that the excitation probability is one, which is justifiable because we performed the experiments at saturation, we can directly deduce the collection efficiency of the setup from the measured count rate. We reached a stable collection efficiency of $\eta = 2.7\,\%$ in saturation, estimated from experimental collection efficiency at 10 MHz laser rate, while having a total single photon count rate of 267 kcts s^{-1} in saturation (see figures 4(b) and (c)).

A more detailed analysis can be based on a simple two-level model. Such a model neglects the metastable singlet (shelving) state of the N-V centre. However, good agreement with respect to the saturation behaviour is obtained. This simple model describes the measured count rate $r(\Gamma)$ as a function of the laser repetition rate Γ. Assuming an excitation probability of one, which is justifiable as explained above, only the collection efficiency η, the lifetime of the emitter γ^{-1} and the laser repetition rate Γ influence the single photon count rate

$$r(\Gamma) = \eta \cdot \Gamma \cdot \gamma \cdot \int_0^{1/\Gamma} \mathrm{e}^{-\gamma t}\,\mathrm{d}t = \eta \cdot \Gamma \cdot (1 - \mathrm{e}^{-\gamma/\Gamma}).$$

We used this model for the fit in figure 4(c) where the count rate in saturation is displayed as a function of the laser repetition rate. From the fit the photon collection efficiency η can be derived. A value of $\eta = 2.6\,\%$ for the total collection efficiency is found in agreement with the estimated η of 2.7 %. This is the highest yet reported collection efficiency for a stable N-V defect centre in diamond. Furthermore, the collection efficiency for the blinking defect centre with

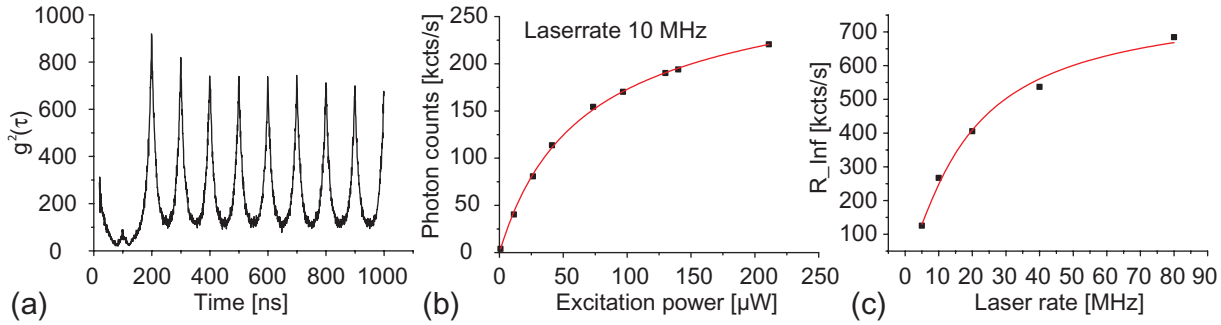

Figure 4. Pulsed autocorrelation function, saturation measurement at pulsed excitation and emission in saturation as a function of laser rate. (a) Pulsed autocorrelation measurement with $g^{(2)}(0) = 0.16$ of the stable, bright emitter depicted in figure 3(a) excited at an excitation intensity of 77 μW with 10 MHz laser rate and count rates of 221 kcts s^{-1}. (b) Saturation curve of the same emitter as in (a) under pulsed excitation of 10 MHz with $R_{\mathrm{Inf}} = 267$ kcts s^{-1} and $I_{\mathrm{Sat}} = 60\,\mu$W. The red curve is a theoretical fit to the data (see text). (c) R_{Inf} as a function of laser repetition rate. The theoretical fit to the data (red curve) is further explained in the text.

count rates up to 2.4 Mcts s^{-1} at CW excitation (see figure 3(b)) was even higher. With a lifetime of 17.6 ns it also emits ultrahigh single photon flux when excited with pulsed laser light. At laser repetition rates of 10 MHz and 385 μW, up to 420 kcts s^{-1} were detected. This determines a collection efficiency of 4.2 % on a timescale of several tens of seconds. The determined setup efficiency η_{Setup} after the flat surface of the SIL of $\eta_{\mathrm{Setup}} < 0.23$ gives a source efficiency ϵ, i.e. the fraction of light collected by the first objective, of $\epsilon > 11.7\,\%$ and $\epsilon > 18.3\%$ for the stable and the blinking defect centre, respectively. η_{Setup} was calculated from reflection and transmission parameters of all optical elements according to their datasheet values and presents the optimistic upper boundary, thus, the source efficiency ϵ is more likely to be higher than estimated here.

The single photon character of the emitters excited with pulsed laser light was also demonstrated by measuring the normalized intensity autocorrelation function $g^{(2)}(\tau)$. Figure 4(a) depicts the pulsed autocorrelation function of the N-V centre with $g^{(2)}(0) = 0.16$ at an excitation intensity of 77 μW and a count rate of 221 kcts s^{-1}. Emission under pulsed excitation generally provides better suppression of background photons compared to CW excitation as excitation radiation is limited to periods when the electron is in the ground state, i.e. can be excited and emits a single photon. The bright blinking defect centre had $g^{(2)}(0) = 0.11$ while excited with laser rates of 10 MHz and 385 μW excitation power.

In conclusion, we report on an experimentally simple but efficient way to strongly enhance the collection of single photons emitted by N-V centres in diamond at room temperature. We integrated a ZrO_2 solid immersion lens with spin-coated nanodiamonds on its flat surface into our confocal microscope. We measured count rates in saturation of up to 853 kcts s^{-1} for a stable N-V centre and up to 2.4 Mcts s^{-1} for a blinking defect centre. Furthermore, our compact SIL design provides access to about 100 N-V centres that emit more than 400 kcts s^{-1}. The overall collection efficiency of our setup is up to 4.2 % while having a source efficiency ϵ of

up to $\epsilon > 18.3\,\%$, opening the way towards much more efficient diamond-based on-demand single photon sources. Furthermore, the setup is versatile and allows the implementation of any kind of defect centre located in a nanodiamond. This is thus very attractive for integration of even brighter emitters with smaller bandwidth. For a single Si-V centre with a lifetime of 1.2 ns as was just very recently presented in [31], we estimate count rates of up to 10 Mcts s^{-1}. As the immersion microscope works oil-free, measurements at cryogenic temperatures will be possible which is mandatory for more complex quantum optical experiments such as two-photon interference.

Acknowledgments

We thank T Aichele for fruitful discussions. We acknowledge financial support from the Federal Ministry of Science and Education (BMBF, project KEPHOSI).

References

[1] O'Brien J L, Furusawa A and Vuckovic J 2009 Photonic quantum technologies *Nat. Photon.* **3** 687–95
[2] Neumann P, Beck J, Steiner M, Rempp F, Fedder H, Hemmer P R, Wrachtrup J and Jelezko F 2010 Single-shot readout of a single nuclear spin *Science* **329** 542–4
[3] Dutt M V G, Childress L, Jiang L, Togan E, Maze J, Jelezko F, Zibrov A S, Hemmer P R and Lukin M D 2007 Quantum register based on individual electronic and nuclear spin qubits in diamond *Science* **316** 1312–6
[4] Bouwmeester D, Pan J W, Mattle K, Eibl M, Weinfurter H and Zeilinger A 1997 Experimental quantum teleportation *Nature* **390** 575–9
[5] Schmid C, Kiesel N, Weber U K, Ursin R, Zeilinger A and Weinfurter H 2009 Quantum teleportation and entanglement swapping with linear optics logic gates *New J. Phys.* **11** 033008
[6] Kuhn A, Hennrich M and Rempe G 2002 Deterministic single-photon source for distributed quantum networking *Phys. Rev. Lett.* **89** 067901
[7] Darquie B, Jones M P A, Dingjan J, Beugnon J, Bergamini S, Sortais Y, Messin G, Browaeys A and Grangier P 2005 Controlled single-photon emission from a single trapped two-level atom *Science* **309** 454–6
[8] Keller M, Lange B, Hayasaka K, Lange W and Walther H 2004 Continuous generation of single photons with controlled waveform in an ion-trap cavity system *Nature* **431** 1075–8
[9] Lounis B and Moerner W E 2000 Single photons on demand from a single molecule at room temperature *Nature* **407** 491–3
[10] Michler P, Kiraz A, Becher C, Schoenfeld W V, Petroff P M, Zhang L, Hu E and Imamoglu A 2000 A quantum dot single-photon turnstile device *Science* **290** 2282–5
[11] Kurtsiefer C, Mayer S, Zarda P and Weinfurter H 2000 Stable solid-state source of single photons *Phys. Rev. Lett.* **85** 290–3
[12] Barnes W L, Björk G, Gérard J M, Jonsson P, Wasey J A E, Worthing P T and Zwiller V 2002 Solid-state single photon sources: light collection strategies *Eur. Phys. J.* D **18** 197–210
[13] Claudon J, Bleuse J, Malik N S, Bazin M, Jaffrennou P, Gregersen N, Sauvan C, Lalanne P and Gerard J M 2010 A highly efficient single-photon source based on a quantum dot in a photonic nanowire *Nat. Photon.* **4** 174–7
[14] Dousse A, Suffczynski J, Beveratos A, Krebs O, Lemaitre A, Sagnes I, Bloch J, Voisin P and Senellart P 2010 Ultrabright source of entangled photon pairs *Nature* **466** 217–20
[15] Simpson D A, Ampem-Lassen E, Gibson B C, Trpkovski S, Hossain F M, Huntington S T, Greentree A D, Hollenberg L C L and Prawer S 2009 A highly efficient two level diamond based single photon source *Appl. Phys. Lett.* **94** 203107

[16] Wang C, Kurtsiefer C, Weinfurter H and Burchard B 2006 Single photon emission from SiV centres in diamond produced by ion implantation *J. Phys. B: At. Mol. Opt. Phys.* **39** 37
[17] Rabeau J R, Huntington S T, Greentree A D and Prawer S 2005 Diamond chemical-vapor deposition on optical fibers for fluorescence waveguiding *Appl. Phys. Lett.* **86** 134104
[18] Wolters J, Schell A W, Kewes G, Nüsse N, Schoengen M, Doscher H, Hannappel T, Lochel B, Barth M and Benson O 2010 Enhancement of the zero phonon line emission from a single nitrogen vacancy center in a nanodiamond via coupling to a photonic crystal cavity *Appl. Phys. Lett.* **97** 141108
[19] Schröder T, Schell A W, Kewes G, Aichele T and Benson O 2011 Fiber-integrated diamond based single photon source *Nano Lett.* **11** 198–202
[20] Beveratos A, Kühn S, Brouri R, Gacoin T, Poizat J-P and Grangier P 2002 Room temperature stable single-photon source *Eur. Phys. J.* D **18** 191–6
[21] Babinec T M, M H J, Khan M, Zhang Y, Maze J R, Hemmer P R and Loncar M 2010 A diamond nanowire single-photon source *Nat. Nanotechnol.* **5** 195–9
[22] Hadden J P, Harrison J P, Stanley-Clarke A C, Marseglia L, Ho Y L D, Patton B R, O'Brien J L and Rarity J G 2010 Strongly enhanced photon collection from diamond defect centres under micro-fabricated integrated solid immersion lenses arXiv:1006.2093v2
[23] Siyushev P *et al* 2010 Integrated diamond optics for single photon detection arXiv:1009.0607v1
[24] Mansfield S M and Kino G S 1990 Solid immersion microscope *Appl. Phys. Lett.* **57** 2615–6
[25] Terris B D, Mamin H J, Rugar D, Studenmund W R and Kino G S 1994 Near-field optical data storage using a solid immersion lens *Appl. Phys. Lett.* **65** 388–90
[26] Koyama K, Yoshita M, Baba M, Suemoto T and Akiyama H 1999 High collection efficiency in fluorescence microscopy with a solid immersion lens *Appl. Phys. Lett.* **75** 1667–9
[27] Lukosz W and Kunz R E 1977 Light emission by magnetic and electric dipoles close to a plane interface. I. Total radiated power *J. Opt. Soc. Am.* **67** 1607–15
[28] Baba M, Sasaki T, Yoshita M and Akiyama H 1999 Aberrations and allowances for errors in a hemisphere solid immersion lens for submicron-resolution photoluminescence microscopy *J. Appl. Phys.* **85** 6923–5
[29] Aharonovich I, Zhou C, Stacey A, Orwa J, Castelletto S, Simpson D, Greentree A D, Treussart F, Roch J F and Prawer S 2009 Enhanced single-photon emission in the near infrared from a diamond color center *Phys. Rev.* B **79** 235316
[30] Steinmetz D, Neu E, Meijer J, Bolse W and Becher C 2010 Single photon emitters based on Ni/Si related defects in single crystalline diamond arXiv:1007.0202v3
[31] Neu E, Steinmetz D, Riedrich-Moeller J, Gsell S, Fischer M, Schreck M and Becher C 2010 Single photon emission from silicon-vacancy centres in CVD-nano-diamonds on iridium arXiv:1008.4736v1
[32] Bradac C, Gaebel T, Naidoo N, Sellars M J, Twamley J, Brown L J, Barnard A S, Plakhotnik A V and Rabeau J R 2010 Observation and control of blinking nitrogen-vacancy centres in discrete nanodiamonds *Nat. Nanotechnol.* **5** 345–9
[33] Ladd T D, Jelezko F, Laflamme R, Nakamura Y, Monroe C and O'Brien J L 2010 Quantum computers *Nature* **464** 45–53